Article

Developmental Cell

Interkinetic Nuclear Migration Is Centrosome Independent and Ensures Apical Cell Division to Maintain Tissue Integrity

Graphical Abstract

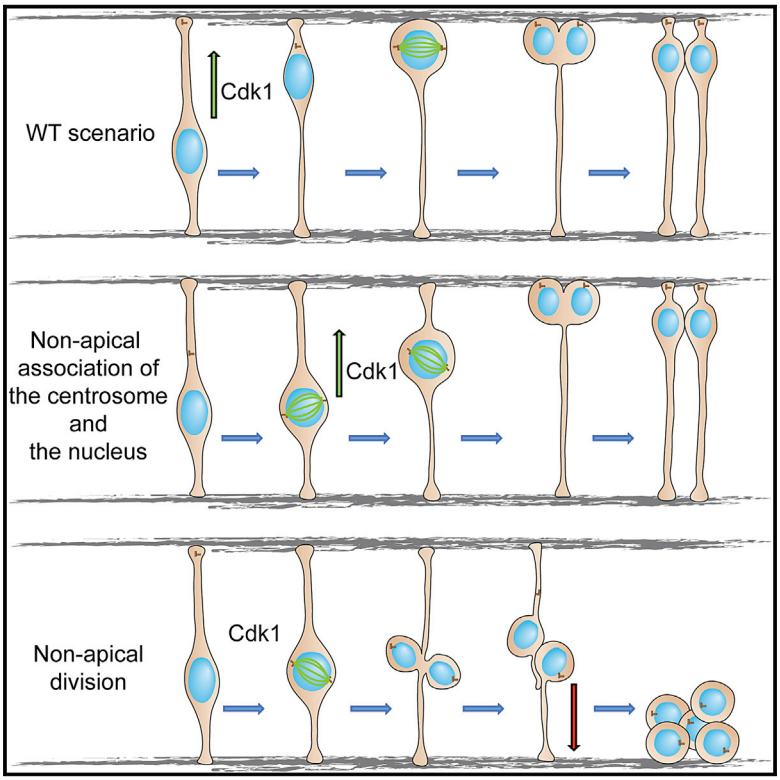

Authors

Paulina J. Strzyz, Hyun O. Lee, ..., Louis C. Leung, Caren Norden

Correspondence

norden@mpi-cbg.de

In Brief

Strzyz et al. show that, in zebrafish, pseudostratified retinal neuroepithelia apical nuclear migration prior to mitosis is a highly reproducible phenomenon. It does not depend on centrosome number, location, integrity, or position of mitotic entry. This ensures that proliferative cells robustly divide apically and safeguards tissue architecture and maturation.

Highlights

- Apical IKNM is highly robust and occurs independently of the centrosome
- CDK1 activity is necessary and sufficient to drive apical IKNM
- Nonapical divisions perturb integrity of the pseudostratified neuroepithelium
- Apical localization of divisions safeguards tissue architecture and maturation

Strzyz et al., 2015, Developmental Cell 32, 203–219
January 26, 2015
http://dx.doi.org/10.1016/j.devcel.2014.12.001

CellPress

Developmental Cell
Article

Interkinetic Nuclear Migration Is Centrosome Independent and Ensures Apical Cell Division to Maintain Tissue Integrity

Paulina J. Strzyz,[1] Hyun O. Lee,[1] Jaydeep Sidhaye,[1] Isabell P. Weber,[1] Louis C. Leung,[1] and Caren Norden[1,*]
[1]Max Planck Institute of Molecular Cell Biology and Genetics, Pfotenhauerstraße 108, 01307 Dresden, Germany
*Correspondence: norden@mpi-cbg.de
http://dx.doi.org/10.1016/j.devcel.2014.12.001

SUMMARY

Pseudostratified epithelia are widespread during animal development and feature elongated cells whose nuclei adopt various positions along the apicobasal cell axis. Before mitosis, nuclei migrate toward the apical surface, and subsequent divisions occur apically. So far, the exact purpose of this nuclear migration remained elusive. One hypothesis was that apical migration ensures that nuclei and centrosomes meet for mitosis. We here demonstrate that in zebrafish neuroepithelia apical nuclear migration occurs independently of centrosome position or integrity. It is a highly reproducible phenomenon linked to the cell cycle via CDK1 activity. We propose that the robustness of bringing nuclei apically for mitosis ensures that cells are capable of reintegrating into the epithelium after division. Nonapical divisions lead to cell delamination and formation of cell clusters that subsequently interfere with neuronal layering. Therefore, positioning divisions apically in pseudostratified neuroepithelia could serve to safeguard epithelial integrity and enable proper proliferation and maturation.

INTRODUCTION

Pseudostratified epithelia (PSE) are found during the development of many organisms. They give rise to various tissues in a wide range of animals, including invertebrates like *Nematostella* and *Drosophila*, as well as vertebrates including zebrafish, chick, rodents, and humans (Grosse et al., 2011; Kosodo et al., 2011; Meyer et al., 2011; Norden et al., 2009; Rujano et al., 2013; Spear and Erickson, 2012). Pseudostratified neuroepithelia (NE) have gathered special attention, as they generate many parts of the nervous system.

Cells within PSE are attached to basal and apical laminae and are highly elongated. Their centrosomes are localized to the apical surface during the whole cell cycle (Miyata, 2008; Norden et al., 2009; Tsai et al., 2010). Cell lengths range from 40–50 μm in NE of zebrafish or the imaginal disk of *Drosophila* (Meyer et al., 2011; Norden et al., 2009) to 250 μm in rodent neocortex (Hu et al., 2013; Kosodo et al., 2011) and up to the millimeter scale in the primate neocortex (Rakic, 1972). Nuclei of these cells locate all along the apicobasal axis resulting in the stratified appearance of the tissue (Lee and Norden, 2013). In the proliferative state, when PSE expand and cells do not yet differentiate, divisions take place at apical positions with cleavage planes perpendicular to the apical surface (Das et al., 2003; Morin et al., 2007; Nakajima et al., 2013; Weber et al., 2014; Xie et al., 2013). It is proposed that such perpendicular division angles are crucial for the maintenance of tissue integrity in the PSE of *Drosophila* imaginal disk (Nakajima et al., 2013) and chick neural tube NE (Morin et al., 2007). In rodent NE, including retina and hindbrain, however, an increase in nonperpendicular divisions has been observed upon the onset of neurogenesis (Cayouette and Raff, 2003; Kosodo et al., 2004).

Apical mitoses observed in all PSE result from apical nuclear migration in G2 (Kosodo et al., 2011; Leung et al., 2011). Following apical division, nuclei are distributed more basally until the completion of S phase, after which they return to the apical side and divide again. This bidirectional movement of nuclei is known as interkinetic nuclear migration (IKNM). Since its initial observation in 1935 (Sauer, 1935), IKNM has been extensively studied in many model organisms and tissues (Grosse et al., 2011; Meyer et al., 2011; Norden et al., 2009; Rujano et al., 2013; Tsai et al., 2010). The cytoskeletal machineries that drive apical IKNM vary depending on tissue type. In shorter epithelia (i.e., NE of the zebrafish or *Drosophila* PSE), forces for moving nuclei are generated by actomyosin contractions (Leung et al., 2011; Meyer et al., 2011; Norden et al., 2009; Rujano et al., 2013). In the more elongated mammalian neocortex, however, mainly microtubules (MTs) and their motors are involved (Hu et al., 2013; Kosodo et al., 2011; Tsai et al., 2010). Collectively, these studies provided substantial mechanistic insights into nuclear kinetics and the cytoskeletal machineries driving IKNM. What is so far less explored though is the basic function of apical IKNM. We further lack an explanation why divisions occur exclusively at the apical surface. One study suggests that apical mitosis is related to the existence of a mitotic zone at the apical endfoot (Hu et al., 2013). According to another hypothesis, apical IKNM is mainly a result of the apical position of centrosomes during interphase, as these organelles are important for spindle formation but also serve as basal bodies for primary cilia (Miyata, 2008; Taverna and Huttner, 2010). Additionally, the position of the nucleus before apical IKNM has been linked to the likelihood of neurogenesis: Two studies provided evidence that the basal depth of nuclei before apical IKNM can be linked to the probability of a neurogenic division in correlation with an

apicobasal Notch/Delta gradient (Baye and Link, 2007; Del Bene et al., 2008). So far, however, all these studies dealt with the process of apical IKNM itself but did not investigate the impact of apical divisions on tissue development and maturation.

Here we set out to explore the importance of apical divisions for tissue maturation in proliferating pseudostratified zebrafish retinal NE. We show that in contrast to recent findings in rodent neocortical PSE (Hu et al., 2013) mitotic entry is not restricted to the apical endfoot. We further demonstrate that the apical localization of the centrosome is not a prerequisite for apical nuclear migration, as apical IKNM still occurs when centrosomes and nuclei meet nonapically or in cases when centrosome integrity is perturbed. Interestingly, apical migration even takes place after nonapical mitotic entry. This finding implies that once apical IKNM is triggered, a ''point of no return'' independent of centrosome position is passed. We find that this upstream trigger is the activation of CDK1, which is necessary and sufficient for the onset of apical IKNM. We also reveal that localizing all mitoses and divisions apically is of general importance for proper proliferation and integrity of pseudostratified NE, as induction of nonapical divisions perturbs retinal development. We therefore suggest that apical migration of nuclei and subsequent apical divisions are mechanisms whose robustness safeguards tissue integrity and thus represents important first steps to orchestrate tissue maturation.

RESULTS

Mitotic Entry Can Occur Nonapically in Zebrafish Retinal NE

We used the developing zebrafish retinal NE to study the occurrence and reproducibility of apical IKNM and apical mitoses in PSE. We first asked whether in zebrafish NE mitotic entry is restricted to the apical endfoot as previously suggested for the rodent neocortex (Hu et al., 2013). If this were the case, apical IKNM would be indispensable for mitotic entry and subsequent divisions. As actomyosin contractions are the main force generators during apical IKNM in zebrafish NE, we blocked actomyosin contractility using the myosin II inhibitor blebbistatin (Norden et al., 2009). Notably, following drug treatment, rounded cells that associated with centrosomes were observed at nonapical locations (Figure 1A). These cells stained positively for the mitotic marker phospho-Histone 3 (pH3), and apical as well as basal processes of cells could be observed, arguing against a pure delamination phenomenon (Figures 1B and 1C).

We conclude that in zebrafish NE mitotic entry is not restricted to the apical zone. This raises the question why nevertheless nuclei migrate apically before mitosis.

Apical IKNM Still Occurs when Nucleus and Centrosomes Meet Nonapically

We next aimed to test the previously raised hypothesis that apical IKNM is a result of the apical location of centrosomes in PSE (Miyata, 2008; Taverna and Huttner, 2010) and mainly serves to bring nuclei and centrosomes into close proximity before division. We first analyzed the nuclear and centrosomal dynamics during the cell cycle using proliferating cell nuclear antigen (PCNA), which unambiguously labels all cell cycle phases (Leung et al., 2011). As seen in the typical example in Figure 1D and Movie S1 (available online), in the zebrafish retinal NE, the centrosome becomes motile only shortly before the nucleus reaches the apical endfoot. On average, the centrosome travels 6.7 μm toward the nucleus (Figure 1E, n = 51 cells, four embryos), similar to results in the rodent neocortex (Hu et al., 2013). This means that centrosomes maintain their apical localization during the whole cell cycle and that the migration of nuclei results in nucleus-centrosome association.

If indeed the main reason for the occurrence of apical IKNM was to ensure that the centrosome and the nucleus meet before division, apical IKNM should not take place when the nucleus and centrosome associate nonapically. To test this idea, we introduced additional nonapical ''centrosomes,'' by interfering with the centriole duplication pathway. To allow for temporal control we used heat shock (HS)-inducible constructs (Clark et al., 2012; Norden et al., 2009). We coexpressed an overstabilized (OS) version of Plk4—the key regulator of the centrosome duplication pathway (Holland et al., 2010) and a dominant-negative (DN) form of Cep152, which perturbs centriolar recruitment of Plk4 (Cizmecioglu et al., 2010; Coelho et al., 2013) (Figure S1A). In cells expressing both constructs fused to the fluorescent protein mKate2, we observed the formation of nonapical centrosome-like structure appearing as mKate2 positive foci that were γ-tubulin positive (Figure 2A). These foci recruited centrin as well as centrosome targeted GFP-PACT (Figures S1B and S1C). Additionally, live imaging of EB3-GFP demonstrated that they can act as microtubule organizing centers (MTOCs) as nonapical MT nucleation was observed (Figures 2B and S1D; Movie S2). Together, this shows that these foci indeed functionally resemble centrosomes.

We next investigated whether the interaction of nuclei with such nonapical centrosomes triggers nonapical mitosis and subsequently impairs apical IKNM. Intriguingly, this was not the case. While we observed MT nucleation emanating from the centrosome-like structures (Figure 2B), nuclei still displayed apical movement with similar kinetics as in the control situation (Figures 3C and 3D; Movie S2). Furthermore, all MTOCs of a cell could often be observed to cluster at the apical surface (Figure S1D). pH3 staining confirmed that mitotic figures localized apically (n = 28 of 29, seven embryos) (Figure 3A). Altogether this demonstrates that enabling the mere interaction between the nucleus and an MTOC at nonapical positions does not perturb apical IKNM.

In the condition in which we induced nonapical centrosomes, however, the apically localized centrosome was still present. Therefore, we could not exclude the possibility that the apical position of this centrosome prompted nuclear migration. To investigate this option, we aimed to induce nonapical centrosome-nuclear association in cells that featured normal centrosome number. We noticed that interference with N-cadherin via a DN construct (Wong et al., 2012), as well as colcemide treatment can lead to nonapical association of centrosomes and nuclei (Figures 2C, 2D, and S2A–S2C). Therefore, we used these approaches to investigate whether nonapical centrosome-nucleus association influences apical IKNM. In both assays, cells kept their apical and basal attachments arguing against mere cell delamination (Figures S2A, S2B, and S2D). Interestingly, in the DN-N-Cadherin as well as the colcemide condition nuclei that got in contact with centrosomes at basal

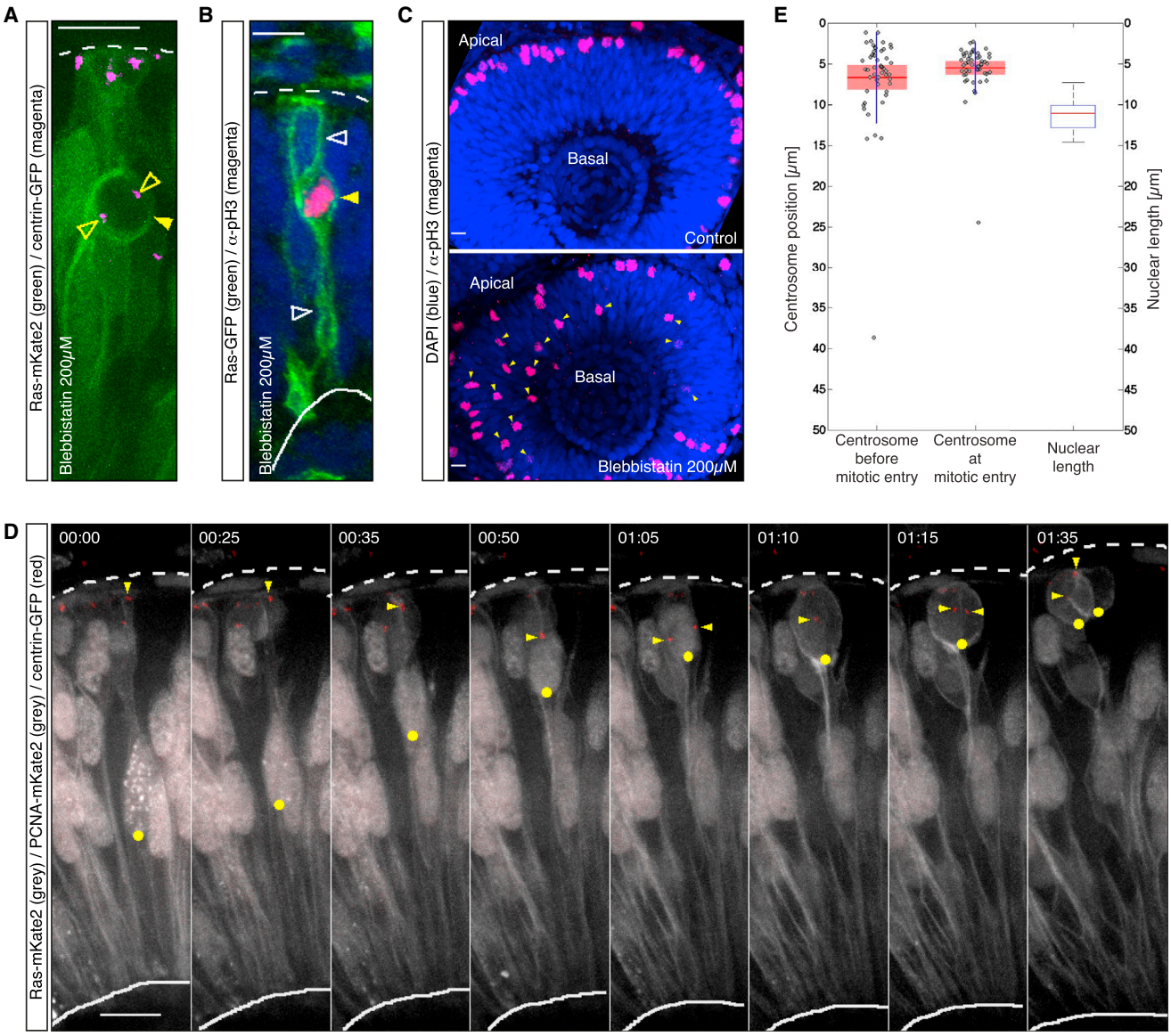

Figure 1. Mitotic Entry Is Not Restricted to the Apical Surface in Zebrafish Retinal NE; Centrosomes Are Maintained Apically throughout the Cell Cycle

(A) Confocal scan of a cell expressing Ras-mKate2 (green) and centrin-GFP (magenta) in an embryo treated with 200 μM blebbistatin 1.5 hr before imaging. The cell shows nonapical mitotic rounding (filled arrow) and is associated with centrosomes (open arrows).

(B) Confocal scan of a cell expressing Ras-GFP (green) stained for pH3 (magenta) in an embryo treated with 200 μM blebbistatin 1.5 hr before fixing. The cell features nonapical pH3 signal (filled arrow) while maintaining apical and basal attachments (open arrows).

(C) Confocal scans of the retinae of an embryo treated with 200 μM blebbistatin 1.5 hr before fixing (lower) and a control embryo (upper) stained for pH3 (magenta). Blebbistatin treated cells enter mitosis nonapically (lower, arrows).

(D) Time-lapse of the dynamics of the nucleus-centrosome pair with respect to cell cycle progression. PCNA-RFP labels nuclei and marks the cell cycle stage (gray). Ras-mKate2 (gray) labels cell membranes. Centrin-GFP (red) labels centrosomes. One nucleus is labeled with a yellow dot. The arrow highlights the position of the centrosome. Time is in hr:min. The frames are from Movie S1.

(E) Centrosome position prior to centrosome splitting (left) and the mean value of the position of centrosomes at mitosis (middle) with respect to nuclear length (right), n = 51 cells, 4 embryos.

Scale bars represent 10 μm. The dotted line represents the apical surface, and the solid line represents the basal side.

positions entered mitosis basally, as demonstrated by the appearance of cell rounding, chromosome condensation, and nuclear envelope breakdown (NEB) (Figures 2C and 2D; Movie S3). Remarkably, however, despite the possibility of nonapical mitotic entry, apical IKNM still occurred. Interestingly, when centrosomes were mispositioned in the DN-N-Cadherin or colcemide condition, apical IKNM typically started shortly before or even after mitotic entry (Figures 2C, 2D, 3E, and 3F). In contrast,

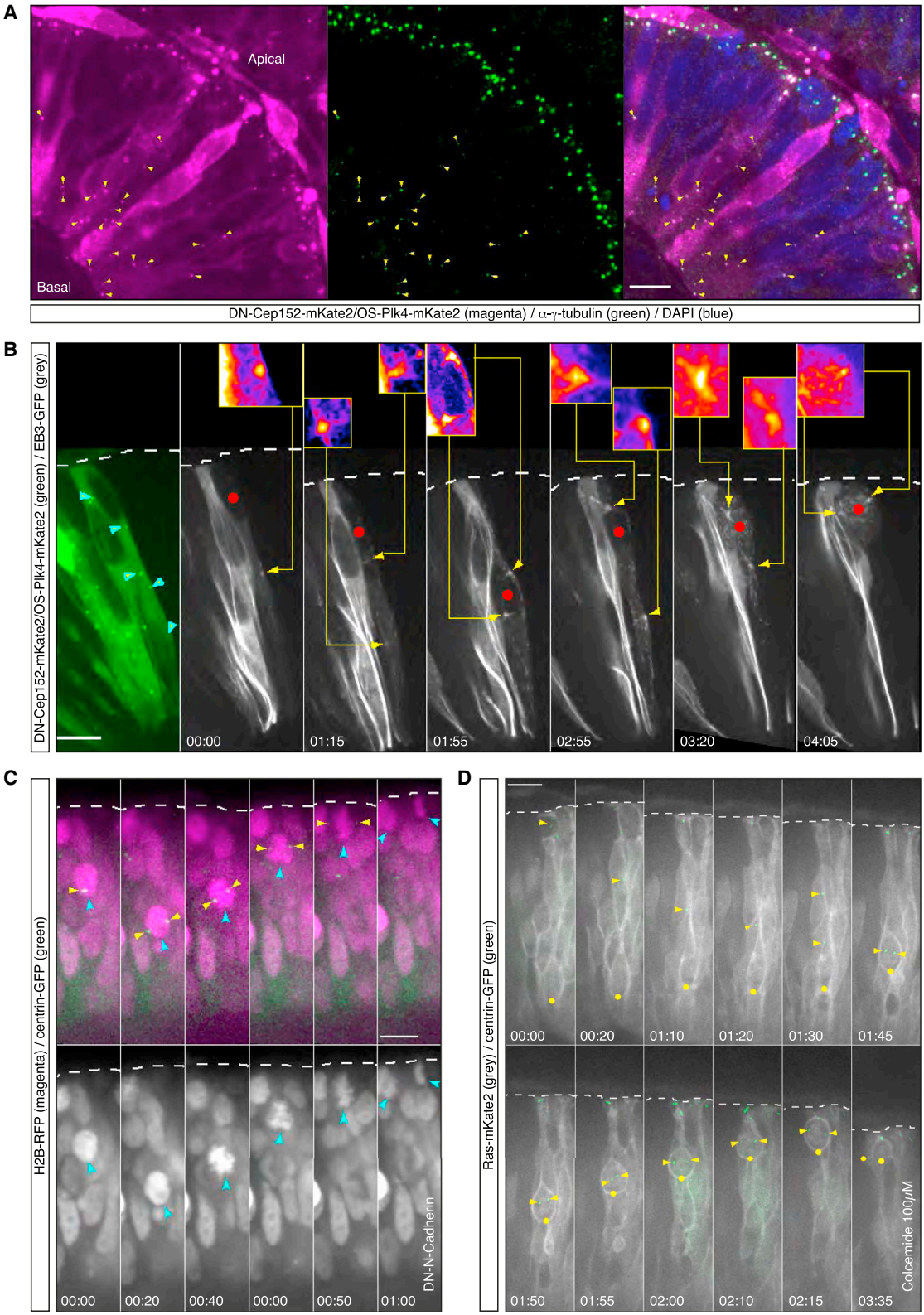

Figure 2. Apical IKNM Persists in Cells in which Centrosomes and Nucleus Meet Nonapically Even following Nonapical Mitotic Entry

(A) Confocal scan of a HS-DN-Cep152-mKate2/HS-OS-Plk4-mKate2 expressing embryo. Positive cells feature cytosolic mKate2 signal as well as foci of signal along the apicobasal axis (magenta). Foci are positive for γ-tubulin staining (green). Nonapical foci positive for mKate2 and immunopositive for γ-tubulin are marked with yellow arrows. HS was performed 8 hr prior to fixing. See also Figure S1.

(legend continued on next page)

in control cells, mitotic entry only took place once the apical side was reached (Figure 3C). pH3 staining of embryos expressing DN-N-Cadherin showed that mitotic figures were found at apical positions (n = 36 of 36, 13 embryos) (Figure 3B). This underlines that even in cases in which centrosome and nuclei can meet nonapically, apical IKNM and apical division still take place. Together this suggests that initiation of apical IKNM occurs independently of apical centrosome position. Additionally, it implies that the apical position of the centrosome cannot be the sole reason for nuclei to migrate apically prior to cell division.

Centrosome Integrity Is Dispensable for Apical IKNM

So far we have demonstrated that apical IKNM is still reproducibly initiated when centrosomes and nuclei associate nonapically. An indication that centrosomes might not be essential for apical nuclear migration in general came from a previous study in *Drosophila*. This study showed that flies without centrioles develop relatively normally (Basto et al., 2006) despite featuring epithelia that display IKNM (Meyer et al., 2011; Rujano et al., 2013). We therefore tested whether centrosomal integrity is a prerequisite for nuclear apical migration in the zebrafish NE. To achieve this, we performed laser ablation of centrosomes in single cells using centrin labeling as a read out. Nuclear dynamics were followed after ablation, and cells were grouped into two categories: (1) cells in which some centrin signal remained but was much weaker and/or more diffuse; these cells most likely featured only remnants of centrosomal material (nine cells, eight nuclei performed apical migration) and (2) cells in which no centrin signal was observed after ablation (five cells, five nuclei performed apical migration). This shows that the vast majority of nuclei following centrosome ablation initiated movement toward the apical side. Some cells subsequently did not progress through mitosis and remained rounded at apical positions (Figure 4A; Movie S4), whereas others managed to complete apical division (Movie S4). Collectively, this argues that even the presence of an intact centrosome is not essential for apical migration of nuclei.

Taken together, in all experimental settings in which we interfered with centrosome position or centrosome integrity, apical IKNM still occurred. This strongly argues that apical IKNM in zebrafish NE is a particularly robust phenomenon that still occurs in challenged conditions independently of apical centrosomes.

Apical IKNM Is Triggered by CDK1 Activity

Our experiments show that apical IKNM is a highly robust phenomenon. Next we wanted to understand how this reproducibility is achieved independently of centrosomes. As IKNM is tightly linked to the cell cycle, we aimed to elucidate the upstream cell cycle components responsible for IKNM robustness and reproducibility. It is known that apical IKNM invariably occurs after completion of S phase, which is in G2 (Kosodo et al., 2011; Leung et al., 2011). Additionally, it is known that cell cycle progression is tightly coordinated by the activity of cyclin-dependent kinases (CDKs) and their associated cyclins (Fisher et al., 2012). Entry into G2 is regulated by the activity of CDK1 in complex with cyclins A or B (Pines and Rieder, 2001). We therefore hypothesized that CDK1 is the cell cycle-associated molecule that controls the timing of apical IKNM. This prediction was supported by results from our previous work showing that cell cycle arrest induced by CDK1 inhibition leads to stalled IKNM (Leung et al., 2011). To reproduce these findings, we used the CDK1 inhibitor RO3306 (Vassilev, 2006). Indeed, upon CDK1 inhibition, cells completed S phase, as indicated by the disappearance of nuclear PCNA foci, but stalled in G2 without initiating apical IKNM (Figures 4C, 4E, and 4F; Movie S5). This is in contrast to controls in which apical IKNM occurred upon the disappearance of nuclear foci (Figures 1D and 4B; Movie S5). This suggested that CDK1 activity is required to induce apical nuclear movements. Next, we explored whether CDK1 activation is also sufficient to trigger apical IKNM. To this end, we made use of the fact that the activity of CDK1 is blocked during S phase due to an inhibitory phosphorylation by Wee1 kinase (Tang et al., 1993). Inhibiting Wee1 activity has been shown to induce precocious CDK1 activity (McGowan and Russell, 1995). To test whether inducing early CDK1 activation prematurely triggers apical IKNM, we inhibited Wee1 using PD0166285 (Leijen et al., 2010). Remarkably, Wee1 inhibition consistently caused nuclear migration to occur already during S phase (Figures 4D–4F; Movie S5), showing that indeed CDK1 activation alone is sufficient to trigger apical nuclear movement independent of cell cycle phase.

Together, our results therefore strongly argue that CDK1 activity is necessary and sufficient to initiate apical IKNM. They also offer an explanation as to why apical IKNM occurs even when nuclei and centrosomes meet nonapically or when centrosome integrity is impaired. Once cells finish S phase, CDK1 activation most likely leads to a "point of no return" for apical movement. Apical IKNM subsequently occurs even in cases in which nuclei already associated with centrosomes and initiated NEB or chromosome condensation nonapically.

(B) Time-lapse of a cell expressing HS-DN-Cep152-mKate2, HS-OS-Plk4-mKate2 (green), and the dynamic MTs marker HS-EB3-GFP (gray). (Left) Cytosolic mKate2 signal and nonapical foci (cyan outlined arrows) in the cell of interest are shown. The remaining panels show distribution of dynamic MTs. Clear foci of nonapical MT nucleation can be observed (yellow arrows). In the insets, magnified regions of nonapical MT nucleation sites are shown in fire lookup table (in panels 4 and 7, 1.5× magnification, remaining panels 3× magnification). The red dot marks the position of the nucleus. HS was performed 12.5 hr prior to time-lapse. Time is in hr:min. The frames are from Movie S2.

(C) Time-lapse of a cell expressing DN-N-Cadherin. HS-H2B-RFP labels nuclei/chromatin (magenta in the upper and gray in the lower) and centrin-GFP-RNA labels centrosomes (green, upper panel only). The centrosome (yellow arrow) associates with the nucleus (cyan, arrow) in a nonapical position (upper). The cell enters mitosis nonapically as visualized by chromosome condensation (lower, 00:40, cyan arrow). Apical IKNM and apical division occur. HS was preformed 17.5 hr prior to time-lapse. Time is in hr:min. The frames are from Movie S2. See also Figure S2.

(D) Time-lapse of a cell in an embryo treated with 100 μM colcemide. The cell expresses Ras-mKate2 (gray) and centrin-GFP (green). In the cell of interest the split centrosome (yellow arrows) travels basally and associates with the nucleus (yellow dot) nonapically. After nonapical cell rounding (01:50), the cell performs apical IKNM. Time-lapse was started 5 hr after drug addition. Time is in hr:min. The frames are from Movie S3.

Scale bars represent 10 μm. The dotted line represents the apical surface.

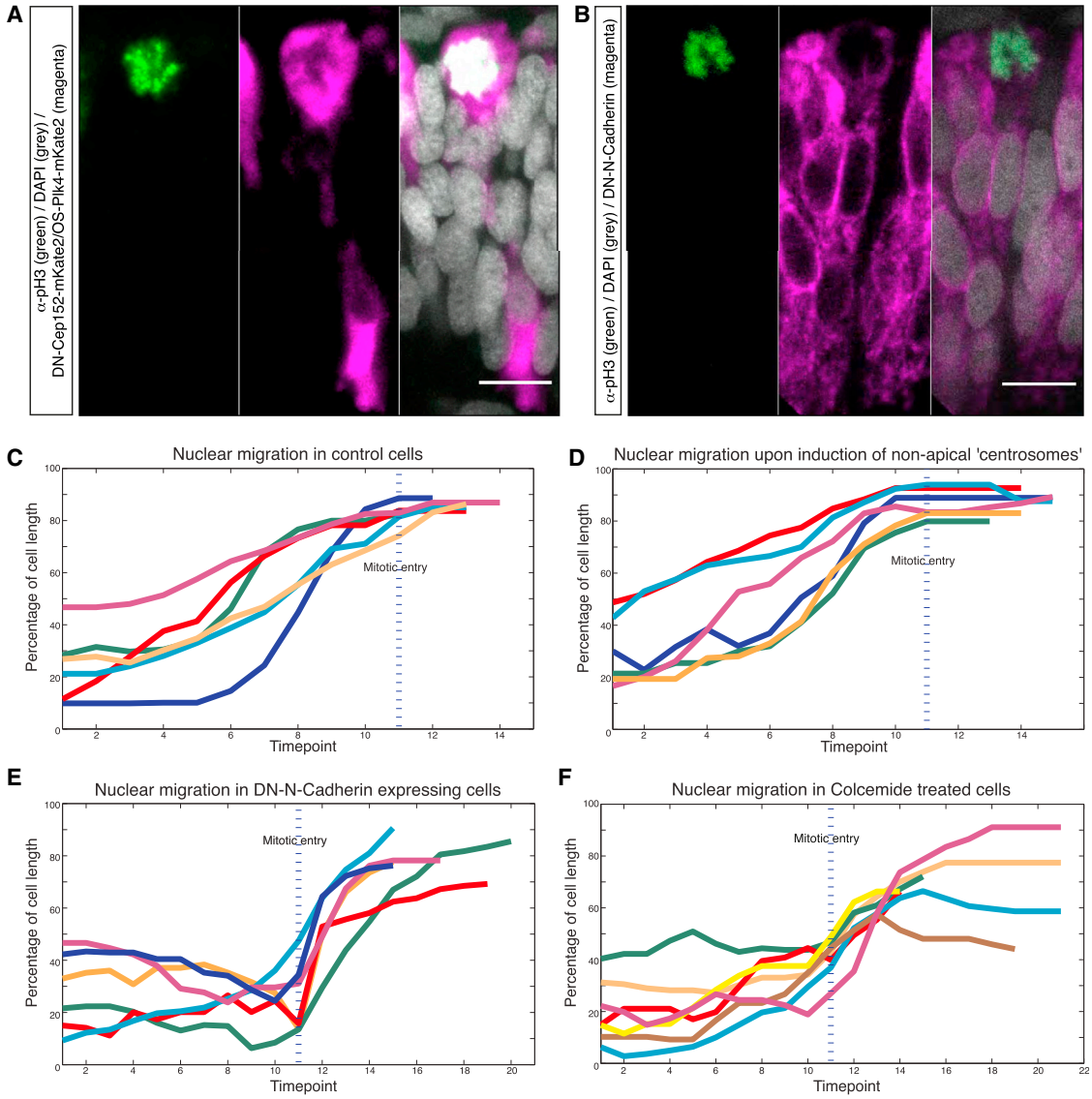

Figure 3. Apical IKNM Persists Despite Nonapical Mitotic Entry

(A and B) pH3 stainings (green) of embryos expressing HS-DN-Cep152-mKate2/HS-OS-Plk4-mKate2 (A) or DN-N-Cadherin (B) (both magenta).

(C–F) Tracks of nuclear position around mitosis in (C) control cells, (D) cells featuring nonapical centrosomes, (E) cells expressing DN-N-Cadherin, (F) cells treated with 100μM colcemide. Time shown in time points (tp). 1 tp = 5 min. Nuclear position was tracked 10 tp (= 50 min) prior to and 10 tp after mitotic entry or until division. Nuclear position has been measured from the base of the nucleus to the basal lamina and was normalized with respect to cell length. Each track represents a single nucleus; tp of mitotic entry is marked with blue line (always at tp = 11).

Scale bars represent 10 μm.

Apical Nonperpendicular Divisions Do Not Perturb Retinal Tissue Architecture and Maturation

At this point, we unveiled that apical IKNM is a particularly reproducible event that depends on CDK1 activity and thereby occurs even in challenged conditions. We next aimed to find out whether the reproducibility of bringing all nuclei apically for division is important for tissue development per se. One possible explanation is that only at apical locations can cleavage planes be precisely controlled leading to perpendicular divisions. In support of this idea, it has been previously suggested that perpendicular cleavage planes are implicated in the maintenance of tissue integrity of *Drosophila* and chick PSE (Morin et al., 2007; Nakajima et al., 2013). Therefore, one assumption was that apical IKNM is a prerequisite for successful tissue development of PSE by enabling the control of cleavage planes at division. To investigate whether this is the case, we examined how interference with apical cleavage planes impacts the integrity of retinal NE. We used previously published morpholinos (MOs) targeting aPKCλ/ζ as these have been shown to induce nonperpendicular divisions (Cui et al., 2007). *aPKCλ/ζ* MOs were injected mosaically into 8- to 32-cell stage embryos together with fluorescently tagged RNAs to label affected cells (Norden et al., 2009). We

observed that divisions took place apically at 34 hours postfertilization (hpf) (Figure 5A). This is in contrast to a previous report using the same MO combination (Cui et al., 2007). The most likely reasons for this discrepancy are differences in effective MO concentration or the fact that we injected MOs at the 8- to 32-cell stage to avoid early morphological defects as opposed to the 1-cell stage in the previous study. In accordance with the work by Cui et al. (2007), however, the clear bias for perpendicular apical cleavages was lost in *aPKCλ/ζ* morphants (Figures 5B and 5C). To ensure that morphant cells did not display marked polarity defects, we performed staining against the tight junction component ZO-1 and confirmed that no differences to control epithelia were found (Figure 5D). We performed live imaging to monitor centrosome and Par3 behavior and observed that after nonperpendicular divisions also the more basal daughter quickly repositioned its centrosome as well as Par3 toward the apical side (Figures 5E and 5F; Movie S6). This confirmed that cells were able to re-establish polarity and reintegrate into the tissue by recreating their bipolar morphology. Subsequently, we investigated whether perturbing apical cleavage planes leads to defects in tissue maturation. To address this issue, we injected *aPKCλ/ζ* MOs into Tg(Ath5:GAP-GFP) embryos. Ath5-promoter-driven membrane-GFP labels the first-born retinal neurons—the retinal ganglion cells (RGCs). We examined the RGC layer to deduce whether early neuronal layer formation was impaired. This was not the case, as RGC layer formation was similar to control embryos in *aPKCλ/ζ* morphants (Figure 5G). Additionally, morphant cells contributed to the RGC layer (Figure 5G). This argues that nonperpendicular apical divisions in the zebrafish retinal NE do not markedly perturb tissue architecture and maturation. Cells arising from such divisions can reintegrate into the developing epithelium and differentiate. Therefore, control of cleavage plane positioning alone does not explain the robustness and reproducibility of apical nuclear migration before division in PSE.

Interference with Actin Distribution Leads to Impaired Apical IKNM and Nonapically Dividing Cells

As we observed that perpendicular cleavage planes are not absolutely mandatory for the maintenance of PSE architecture, we speculated that the apical position of divisions itself provides relevant advantages for PSE development. To test this idea, we wanted to explore how nonapical divisions influence tissue development and maturation. To achieve this, we needed a condition that interfered with apical motion of nuclei without blocking cytokinesis (as direct blocking of the actomyosin machinery would) or cell cycle continuation (as this would not allow cell division). We and others recently showed that actomyosin accumulations basal to the nucleus can be linked to the occurrence of apical IKNM (Leung et al., 2011; Rujano et al., 2013). Actomyosin distribution in epithelial cells has been previously shown to be regulated by aPKC in various contexts (Even-Faitelson and Ravid, 2006; Kishikawa et al., 2008; Uberall et al., 1999). Interestingly, in the elongated cells of the pseudostratified epithelium, aPKC is confined to the apical side and does not occur at basolateral locations (Clark et al., 2012). Therefore, we hypothesized that altering aPKC distribution in these cells could influence actomyosin organization and might thus perturb nuclear migration. To test this idea, we used a HS-inducible construct in which aPKC was linked to a CAAX domain, thus targeting the protein to the membrane (Ossipova et al., 2007). Induction of this construct led to a gross alteration of aPKC distribution. The protein was observed to localize to cell membranes apically as well as all along the apicobasal cell axis (Figures 6B and 6C). Because of the involvement of aPKC in epithelial cell polarity, we investigated whether polarity components still localized correctly to the apical membrane in cells expressing aPKC-CAAX. To this end, we first analyzed Par3 localization in these cells. We coinjected a HS-inducible Par3-GFP together with HS-aPKC-CAAX-mKate2 or membrane bound HS-Ras-mKate2 as a control. In both cases, some residual nonapical signal of Par3 was observed (Figures S3A and S3B). This is explained by the fact that HS induction most likely leads to some protein overexpression. Nevertheless, the bulk of Par3 signal was localized to a distinct apical domain both in aPKC-CAAX and control cells (Figures S3A and S3B). Additionally, we stained aPKC-CAAX-expressing cells against the tight junction marker ZO-1. ZO-1 signal was found apically and colocalized with apical Par3 (Figure S3C). We next tested whether aPKC distribution all along the cells' apicobasal axis interfered with actomyosin organization. We visualized F-actin by mosaically expressing the Calponin homology domain of Utrophin, Utr-GFP, which binds F-actin without stabilizing it (Burkel et al., 2007). In the control situation, F-actin was organized as filaments along the apicobasal axis of cells (Figure 6A). This is in accordance with our earlier observations (Leung et al., 2011; Norden et al., 2009). Interestingly, when we expressed aPKC-CAAX, actin filament organization was disrupted, and the signal was more diffuse than in the control condition (Figure 6B). This argues that aPKC-CAAX interferes with actin organization and might thereby represent a valid tool to impair apical IKNM and induce nonapical divisions. We next assessed the cell division positions in aPKC-CAAX-expressing cells. Already at 30 hpf/6 hr post HS (hphs), about a third of all dividing aPKC-CAAX-positive cells (27%, n = 26 cells, 11 embryos) divided at ectopic basal locations. As expected, these nonapical divisions featured randomized cleavage planes (Figure 6D).

These results show that in aPKC-CAAX-expressing cells the interference with actin organization can indeed lead to impaired apical IKNM, which in turn results in a significant amount of nonapical divisions.

The Offspring of Nonapically, Nonperpendicularly Dividing Cells Perturbs Retinal Tissue Maturation

We next tested the impact of nonapical divisions of aPKC-CAAX-expressing cells on tissue development and retinal maturation. Interestingly, before and during division, cells showed bipolar morphology, arguing against delamination (Figures 6C, 6E, 6F, and S3D). Following division, the apical daughter was still integrated in the epithelium, while the basal daughter lost the apical attachment and displayed protrusive activity (Figure 6C; Movie S7). This implied that following nonapical division the ability of the more basal daughter to reintegrate into the epithelium was impaired. To substantiate this finding, we monitored centrosome behavior and Par3 distribution in nonapically dividing aPKC-CAAX-positive cells. We demonstrated that while the apical daughter could reposition the centrosome to the apical surface following division, this process was inefficient in the basal daughter (Figures 6E and S3D; Movie S7). Similarly, the apical

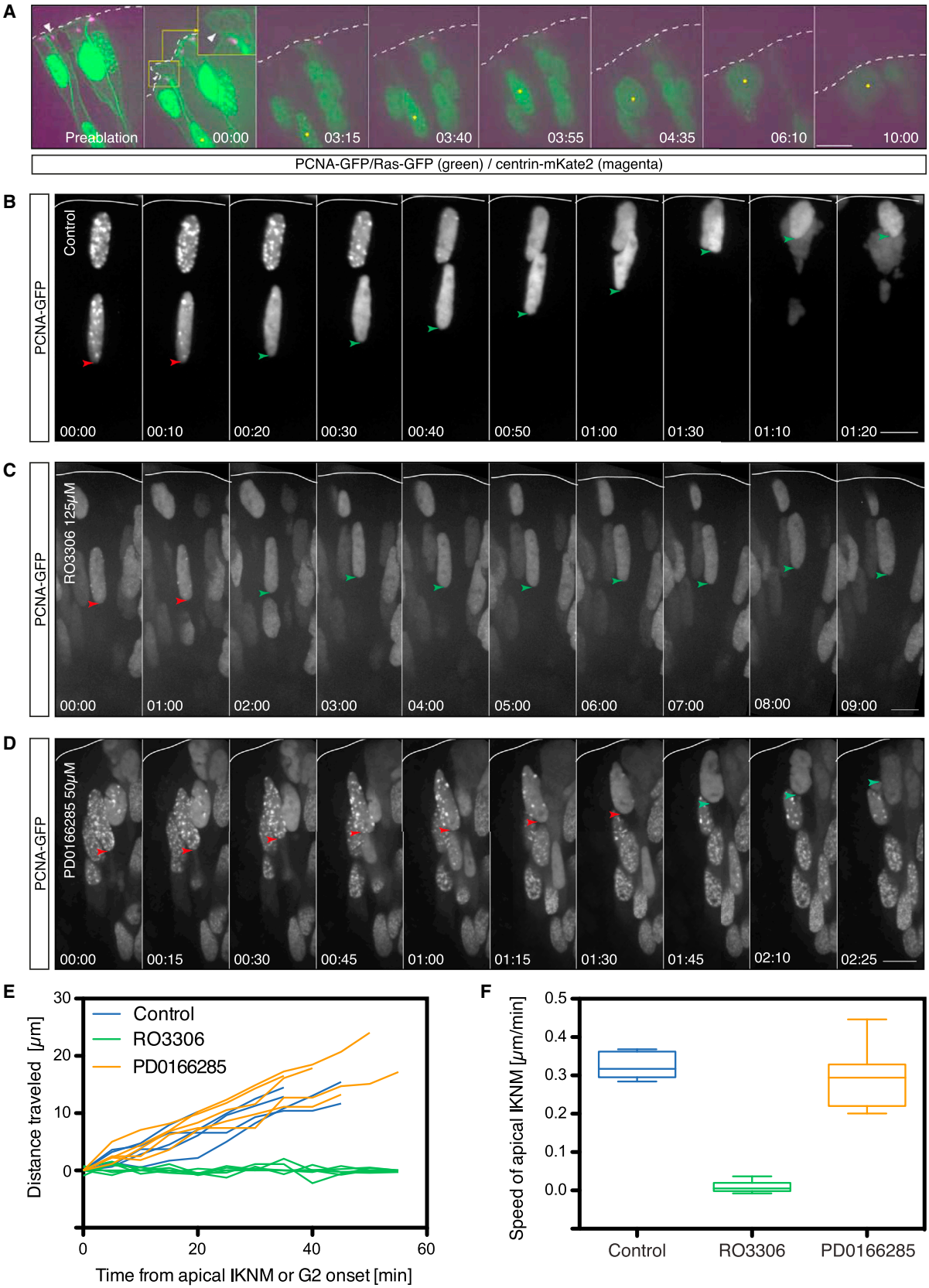

(legend on next page)

daughter inherited apical Par3 signal, maintained during division, while the basal daughter created an ectopic Par3 domain (Figure 6F; Movie S7). In sum, these data show that apical process regrowth and re-establishment of radial morphology are not efficient in more basal daughters of nonapical, nonperpendicular divisions, and consequently, such cells cannot robustly reintegrate into the epithelium.

Subsequently, we tested the effect of nonapical divisions later in development. Notably, at 24–30 hphs, aPKC-CAAX-expressing cells were observed at ectopic basal positions, forming clusters of rounded cells. These cells continued proliferating, as demonstrated by pH3 staining (Figure 7A). We next explored how such basal cell cluster formation affects tissue maturation and architecture. To this end, we injected aPKC-CAAX into Tg(Ath5:GAP-RFP) embryos. Remarkably, Ath5 expression was not observed in aPKC-CAAX-positive cell clusters, while neighboring control cells differentiated normally into RGCs (Figure 7B). These RGCs had to arrange around the aPKC-CAXX positive clusters, resulting in holes in the RGC layer (Figure 7B, lower). This demonstrates that basal cluster formation of cycling aPKC-CAAX-expressing cells negatively impacts retinal development and tissue formation.

To ensure that what we observed for basal divisions in the aPKC-CAAX condition was a general phenomenon, we aimed to induce such divisions in otherwise nonperturbed cells. To this end, we made use of the known fact that inhibition of Plk1 leads to a mitotic arrest (Lénárt et al., 2007). Thereby an accumulation of rounded cells that are stalled in mitosis forms a steric hindrance at the apical surface (Weber et al., 2014). After this boundary has been formed, cells undergoing apical IKNM cannot reach the apical surface leading to nonapical mitotic entry of these cells (Weber et al., 2014). To inhibit Plk1 activity, we here used a genetic approach and expressed a DN construct under HS promoter (Smits et al., 2000). DN-Plk1 was expressed in a subset of cells (marked by additional expression of H2B-RFP), leading to the formation of rounded apical cells stalled in mitosis that blocked the apical surface (Figure 7C). We chose embryos in which we detected such blocking of the apical surface for live imaging. In all embryos imaged, we observed that beneath the blocked apical layer, unperturbed control cells labeled by H2B-GFP and ras-GFP mRNA injection indeed performed nonapical divisions shown by pH3 staining and live imaging (Figures 7C, 7D, and S4A; Movie S8). Interestingly, early after the formation of the apical hindrance, divisions occurred close to the barrier, and cells still featured an apical process during division (Figure 7D, upper). Later, however, the offspring of these cells also divided at very basal positions (Figures 7D, lower, and S4A), arguing that they could not reintegrate into the epithelium, as seen in the aPKC-CAAX condition. We next tested whether also in this condition RGC layer formation can be disturbed. Like in the aPKC-CAAX condition, we used the Tg(Ath5:GAP-GFP) line as a read out. Here we had to fix the embryos without knowing in which ones the access to the apical surface had been sufficiently blocked earlier in development. Nevertheless, we found different embryos that showed basal cluster formation. Like in the aPKC-CAAX condition, holes in the Ath5 layer were observed that contained pH3-positive cells. Additionally, as seen previously, these proliferating cell clusters disturbed neuronal layer formation (Figures 7E, S4B, and S4C).

Together, these results strongly argue that the occurrence of nonapical divisions can be linked to perturbations of PSE integrity leading to defects in tissue maturation. Therefore, we suggest that the remarkable reproducibility of apical IKNM and subsequent apical divisions serves to safeguard tissue integrity and maturation in proliferative zebrafish NE.

DISCUSSION

In this study, we investigated the purpose and significance of localizing divisions to the apical surface in zebrafish NE. We revealed that (1) mitotic entry is not restricted to apical positions, (2) apical IKNM depends on CDK1 and occurs independently of centrosome position or integrity, (3) nonperpendicular apical divisions are tolerated and do not cause tissue perturbations, (4) after nonapical, nonperpendicular divisions caused by interference with actomyosin distribution or steric hindrance at apical locations, cells fail to efficiently reintegrate into the tissue; they instead establish proliferative basal cell clusters that perturb overall tissue maturation. Figure 8 presents a schematic summary of these findings.

Apical Migration Occurs Independently of Centrosome Position and Integrity, as well as Mitotic Entry

It was recently suggested that in the highly elongated cells of the rodent neocortical PSE, mitotic entry is restricted to the apical terminus (Hu et al., 2013). In the zebrafish retinal NE, however, mitotic entry occurred at nonapical positions when the IKNM machinery was inhibited or when centrosomes and nuclei met basally. Our observation is in accordance with a recent study reporting that nonapical mitotic entry can take place also in the PSE of the *Drosophila* imaginal disk (Liang et al., 2014). Interestingly, we documented that apical migration persisted despite mitotic entry at basal locations and even upon perturbing centrosome integrity. We further show that CDK1

Figure 4. Apical IKNM Does Not Depend on Centrosome Integrity; CDK1 Activity Is Necessary and Sufficient for Apical IKNM

(A) Time-lapse imaging of a cell following laser ablation of the apical centrosome. (Left-most panel) Cell prior to ablation. The nucleus is labeled with PCNA-GFP (green). The membrane is visualized with Ras-GFP (green) and the centrosome with centrin-mKate2 (magenta, white arrow). After ablation (00:00), no centrin signal can be detected in the apical process (white arrow). The yellow box in panel 00:00 shows a 2× magnified region of the apical endfoot. The following panels show nuclear behavior following ablation marked by a yellow arrow. Time is in hr:min. The frames are from Movie S4. See also Figure S2.

(B–D) Time-lapse of cells expressing PCNA-GFP (gray) upon treatment with (B) DMSO only, (C) CDK1 inhibitor (RO3306), (D) Wee1 inhibitor (PD166285). Red arrows mark cells in S-phase (PCNA dots), and green arrows mark cells in G2 (disappearance of PCNA dots). Time is in hr:min. The frames are from Movie S5.

(E) Tracks of nuclear movements in the different drug conditions starting at the onset of apical IKNM (PD0166285), the entry into G2 phase (RO3306), or both (control).

(F) Average speed of apical nuclear migration in different conditions. Speed was calculated as total distance traveled by nuclei over time (μm/min). Error bars represent SEM.

Scale bars represent 10 μm. Apical surface is represented by a dotted line in (A) and a solid line in (B)–(D).

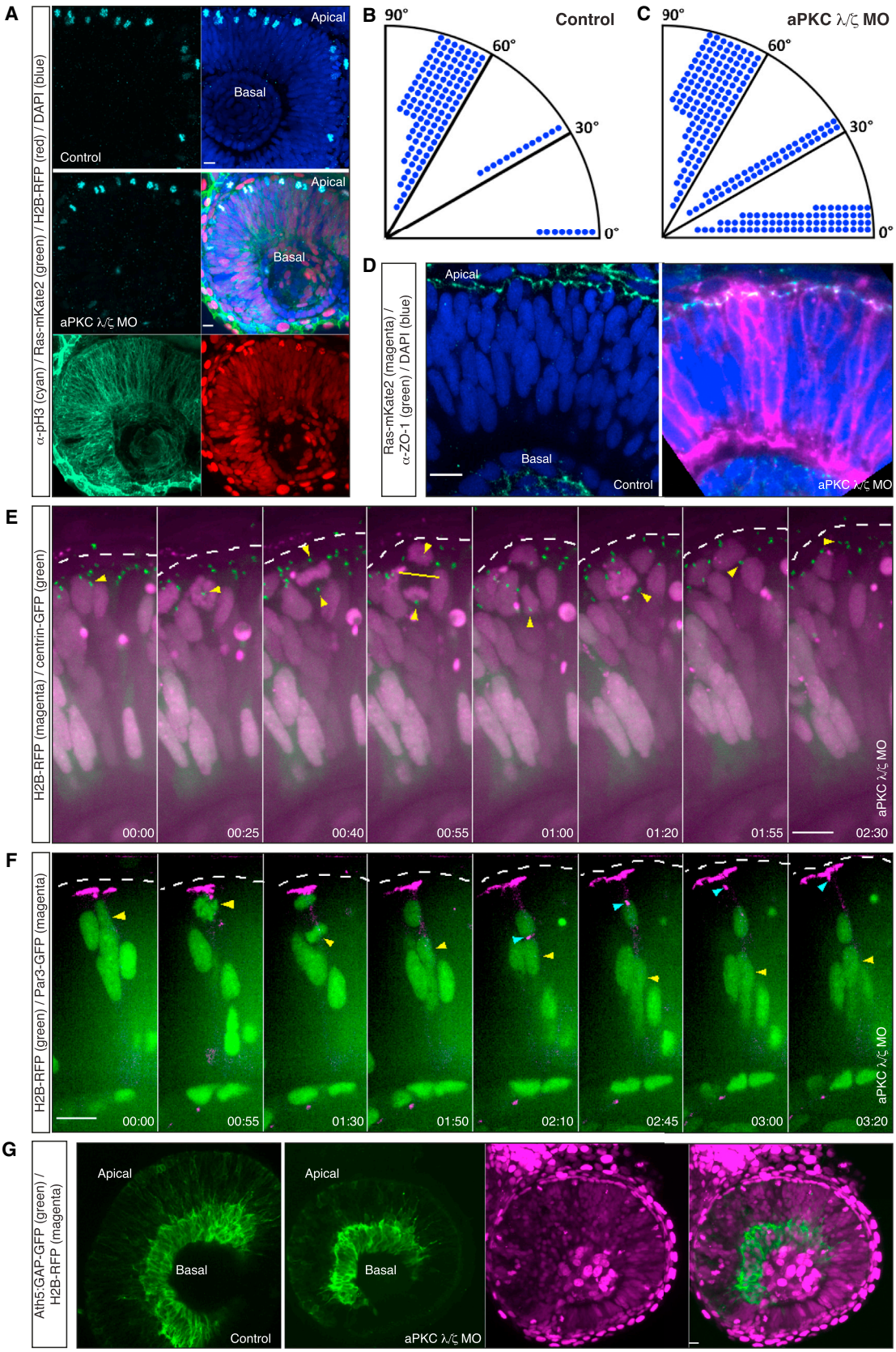

(legend on next page)

activity is necessary and sufficient for apical IKNM. We conclude that once CDK1 is activated the actomyosin machinery passes a point of no return. This drives apical IKNM independently of centrosome number or location and even in cases when the centrosome and the nucleus already met nonapically and mitotic entry was initiated.

Nonapical, Nonperpendicular Divisions Induce Cell Delamination and Result in Perturbed Retinal Architecture

The induction of nonapical divisions was achieved by the expression of membrane-targeted aPKC or due to an apical steric hindrance by cells overexpressing DN-Plk1. These nonapical divisions subsequently impaired the capability of cells to reintegrate into the epithelial tissue, consequently causing their delamination. Offspring of such divisions continued to proliferate ectopically, forming cell clusters that obstructed correct neuronal layer formation and led to overall tissue disorganization. These data strongly suggest that it is indeed the nonapical localization of divisions that impedes cellular reintegration and thereby perturbs tissue integrity and maturation as well as neuronal layering.

It should be noted again here that our studies explore *the proliferative phase* in retinal NE development during which cell divisions exclusively expand the progenitor pool. We believe that ensuring that all divisions occur apically is especially crucial during this period. At later stages of retinal development, however, when neurogenesis peaks, nonapical divisions occur and are well tolerated, giving rise to horizontal and bipolar retinal neurons (Godinho et al., 2007; Weber et al., 2014). We believe that this is due to the fact that at this stage cells are already committed to a neuronal fate. Thus, location of division might not be as important as in the proliferative state, as these daughter cells do not have to reintegrate into the neuroepithelium but become differentiated neurons. This notion is substantiated by the fact that in retinal development nonapical divisions give rise to two daughters of the same fate (Weber et al., 2014). Also in neocortical development, nonapical (here called basal) progenitors exist (Fietz and Huttner, 2011). Divisions of these cells also lead to two daughter cells that do not need to reintegrate into the epithelium. Therefore, nonapical divisions in this scenario do not influence epithelial integrity per se.

Altogether, our data indicate that the successful reintegration of daughter cells into the epithelium in the developing pseudostratified NE before the onset of neurogenesis safeguards proper tissue architecture. Additionally, it is possible that the maintenance of bipolar cell morphology and nuclear oscillations during IKNM also plays a role in cell fate specification. It was hypothesized that a Notch/Delta gradient, observed along the apicobasal axis of chick and zebrafish NE, is important for cell fate decisions (Del Bene et al., 2008; Murciano et al., 2002). As a consequence of this gradient, nuclei adopting different positions along the apicobasal axis are differentially exposed to the signaling cues. In line with this argument, it was shown in retinal NE that a correlation between the apicobasal position of the nucleus and cell fate specification exists (Baye and Link, 2007). This implies that the maintenance of cellular attachments of progenitors in the NE enabling nuclei to migrate along the apicobasal axis of the tissue also plays a role in proper cell differentiation and subsequent fate decisions and tissue maturation.

Collectively, we here present evidence that apical localization of cell divisions is important to guarantee development of the pseudostratified NE into a highly organized tissue. One possible explanation is that reintegration of progenitor daughter cells into the epithelium is facilitated only at this location. Therefore, apical migration during IKNM leading to apical division is an important first step to orchestrate the highly complex stages of tissue maturation in pseudostratified NE.

EXPERIMENTAL PROCEDURES

Zebrafish Husbandry

WT AB, WT TL, as well as Tg(Ath5:GAP-GFP/RFP) (Poggi et al., 2005) were used. Zebrafish were maintained and bred at 26.5°C. Embryos were raised at 28°C. Embryos were treated with 0.003% phenylthiourea (Sigma) from ~8 hpf to prevent pigmentation. All animal work was performed in accordance with European Union (EU) directive 2011/63/EU as well as the German Animal Welfare Act.

Visualizing Intracellular Structures and Modifying Protein Function

Mosaic expression of fluorescently labeled proteins was ensured by the injection of RNA-XFP constructs into one of the blastomeres. This enabled the analysis of subcellular components in single cells. For mechanistic insights into protein function, DN and OS versions of proteins under a HS promoter were used (Clark et al., 2012; Norden et al., 2009). To knock down proteins, we used injection of MOs.

Figure 5. Nonperpendicular Apical Divisions Do Not Majorly Perturb Retinal Tissue Architecture and Early Neuronal Layering

(A) Images of *aPKC λ/ζ* MO-injected embryo (middle and lower) and a control embryo (upper). Ras-mKate2 RNA (green) and H2B-RFP RNA (red) were injected to visualize morphant cells together with MOs. Embryos were fixed at 34 hpf and stained with pH3 antibody to visualize mitotic cells (cyan). In control and morphant embryos, mitoses occur apically.

(B and C) Division angles of the control (B) and *aPKC λ/ζ* morphant cells (C). Dots indicate individual cells. In morphant cells, the clear bias for perpendicular divisions (angles 60°–90°) is lost. (B) n = 145 cells, 7 embryos; (C) n = 241 cells, 8 embryos.

(D) Confocal images of a control (left) and an aPKC λ/ζ morphant embryo (right). Ras-GFP RNA (magenta) was injected together with MOs to visualize morphant cells. Embryos were fixed at 34 hpf and stained with ZO-1 antibody (green). In both cases, ZO-1 signal appears as a continuous apical belt.

(E) Time-lapse of an *aPKC λ/ζ* morphant embryo coinjected with H2B-RFP RNA (magenta) and centrin-GFP RNA (green). Morphant cell divides horizontally (00:55, yellow bar). The more basal centrosome (yellow arrow) descends to the apical surface. Time is in hr:min. The frames are from Movie S6. See also Figure S2.

(F) Time-lapse of an *aPKC λ/ζ* morphant embryo coinjected with H2B-RFP RNA (green) and Par3-GFP RNA (magenta). Morphant cell divides horizontally (01:30). The more basal daughter (yellow arrow) re-establishes its apical Par3 domain (cyan arrow). Time is in hr:min. The frames are from Movie S6.

(G) Early neuronal layer, RGC (marked by Tg(Ath5:GAP-GFP), green) layer in a control embryo (left-most panel) and an *aPKC λ/ζ* morphant embryo (remaining panels). Morphant cells were marked by coinjection of H2B-RFP RNA (magenta). Both in the morphant and the control embryo an intact RGC layer (green) is formed next to the lens. Morphant cells (magenta) contribute to this layer (rightmost panel).

Scale bars represent 10 μm. The dotted line represents the apical surface.

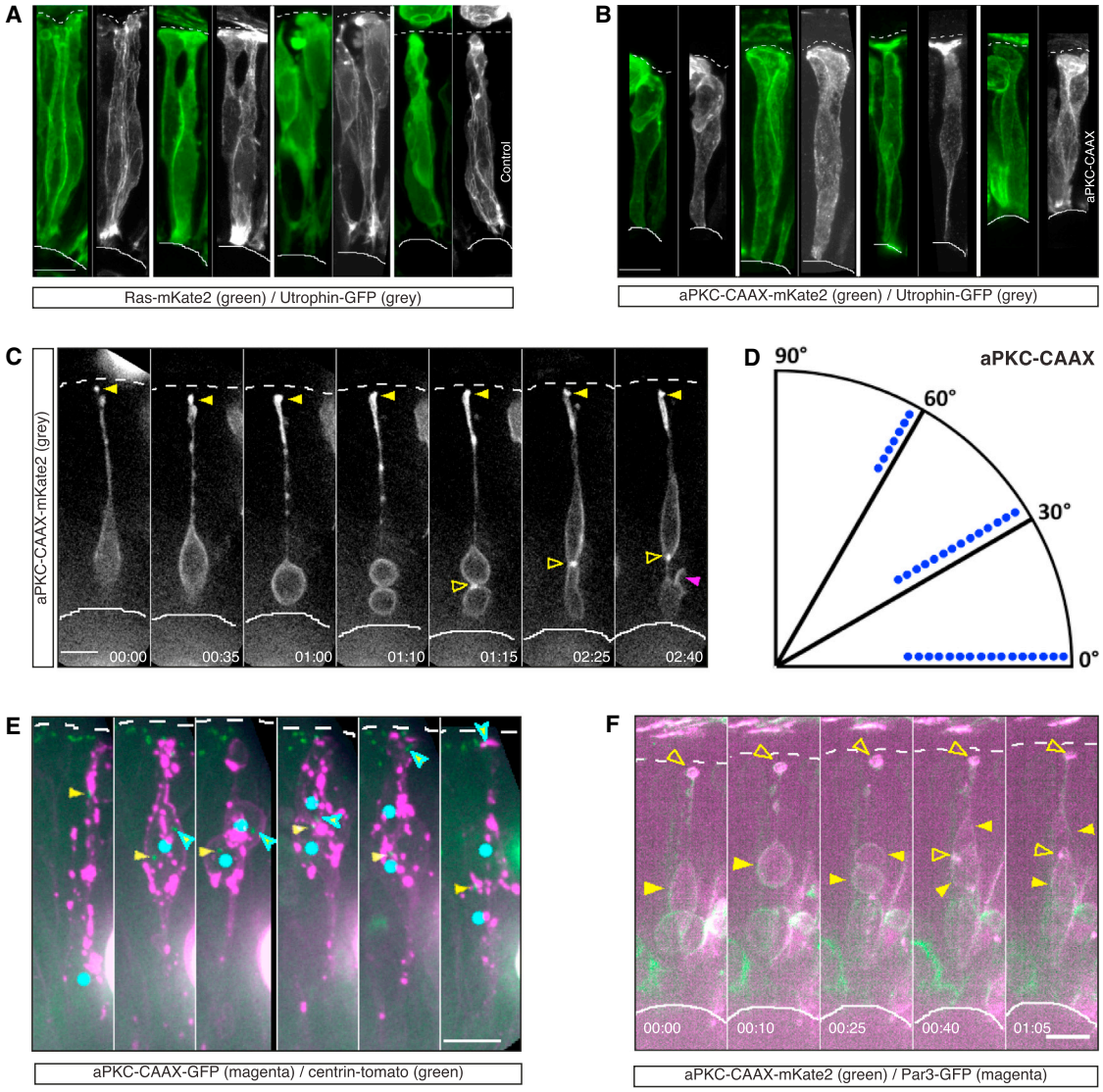

Figure 6. Interference with Actin Distribution via Membranous Expression of aPKC-CAAX Leads to Nonapical Divisions

(A) Confocal scans of actin organization in control cells. Cells were coinjected with HS-Ras-mKate2 (green, membrane) and HS-Utrophin-GFP (F-actin, gray). Actin is organized in distinct filaments. HS was performed 7 hr prior to fixation.

(B) Confocal scans of actin organization in HS-aPKC-CAAX-mKate2 (green) expressing cells coinjected with HS-Utrophin-GFP (F-actin, gray). Actin is diffusely organized without a clear filamentous structure along the cell membrane, despite a clear apical signal. HS is 7 hr prior to fixation.

(C) Time-lapse of a cell expressing aPKC-CAAX-mKate2 (gray). The cell divides nonapically with a horizontal cleavage plane (01:10), while maintaining its apical attachment (yellow filled arrow). The more apical daughter cell maintains its apical process attachment, while the more basal daughter forms an ectopic connection to the sister cell (open arrow). Later, the basal daughter shows protrusive activity (magenta arrow). HS was performed 9.5 hr prior to time-lapse. Time is in hr:min. The frames are from Movie S7. See also Figure S3.

(D) Division angles of the aPKC-CAAX expressing cells dividing nonapically. Dots indicate individual cells. Cells lose clear bias for perpendicular divisions (angles 60° to 90°) observed in controls (Figure 5B), n = 37 cells, 8 embryos.

(E) Time-lapse of a cell expressing HS-aPKC-CAAX-GFP (magenta) and centrin-tomato (green). The cell divides nonapically with a nonperpendicular cleavage plane (02:35). The centrosome of the more apical daughter (cyan-outlined arrow) descends to the apical surface. The centrosome of the more basal daughter (yellow arrow) remains basally. Blue dots represent soma/nuclear position. HS was performed 11.5 hr prior to time-lapse. Time is in hr:min. The frames are from Movie S7. See also Figure S3.

(F) Time-lapse of a cell expressing HS-aPKC-CAAX-mKate2 (green) and HS-Par3-GFP (magenta). The cell divides nonapically with a horizontal cleavage plane (00:25), while maintaining apical process and apical Par3 signal (open arrow). Later, the basal daughter forms an ectopic, basal Par3 domain (open arrow). HS was performed 8 hr prior to the time-lapse. Time is in hr:min. The frames are from Movie S7.

Scale bars represent 10 μm. The dotted line represents the apical surface, and the solid line represents the basal side.

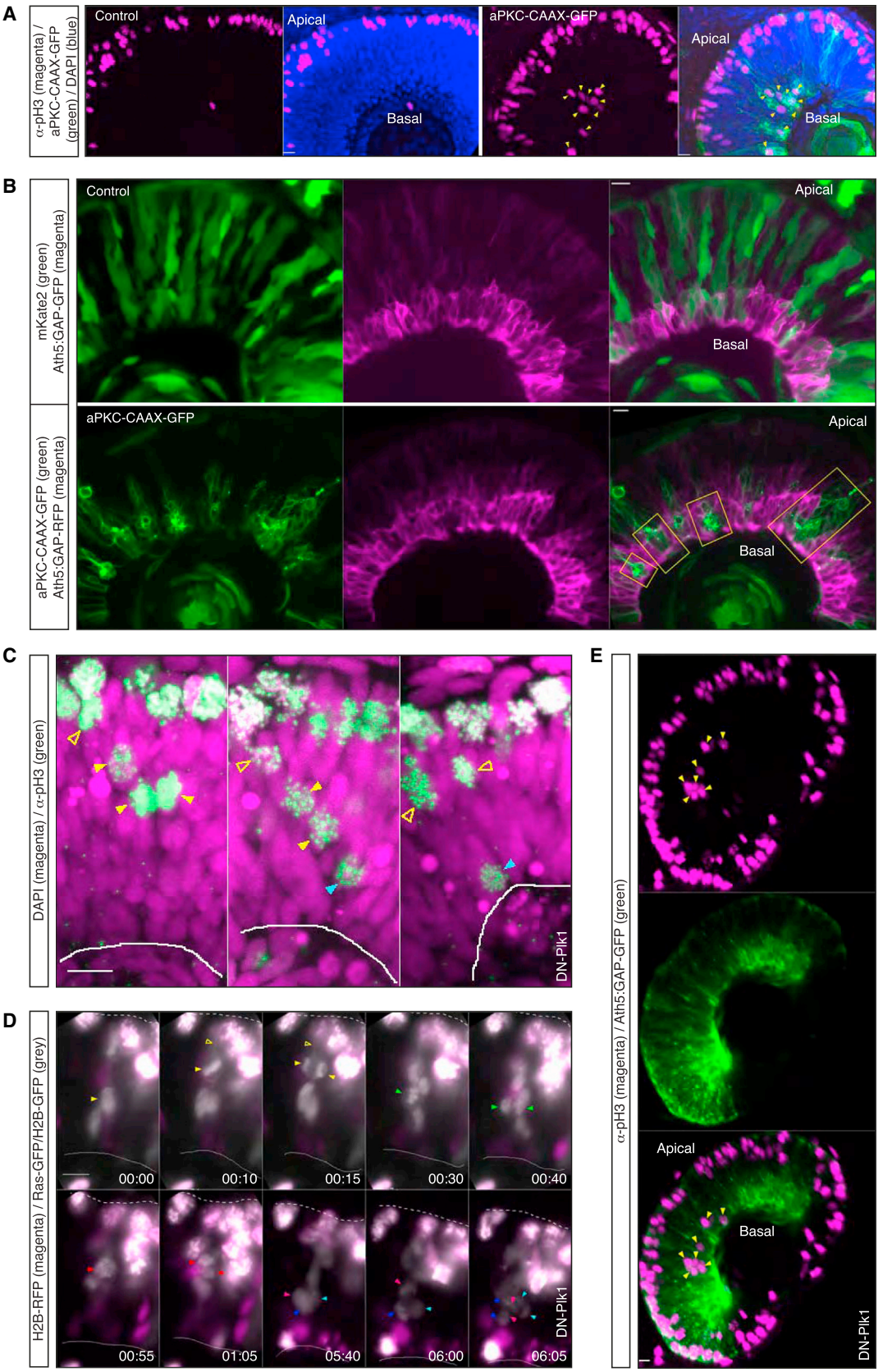

(legend on next page)

RNA Injection

RNA was synthesized using the Ambion SP6 mMessage Machine kit. RNA was injected in volume of 0.3–0.6 nl into one or two cells of 16- to 128-cell stage embryos. RNA concentrations used were between 50 and 125 ng/μl per construct.

DNA Injection

0.5 to 1 nl of DNA constructs was injected into the cytoplasm of one-cell stage embryos. The DNA concentrations used ranged between 10 and 20 ng/μl (HS-EB3-GFP, 1–5 ng/μl).

MO Injection

The following MOs (GeneTools) and their concentrations were used:

aPKC λ MO: 5′-TGTCCCGCAGCGTGGGCATTATGGA-3′ (2 mg/ml)
aPKC ζ MO: 5′-GATCCGTTACTGA-CAGGCATTATA-3′ (3 mg/ml)
p53 MO: 5′-GCGCCATTGCTTTGCAAGAATTG-3′ (3 mg/ml)

Together with MOs, fluorescently tagged RNAs were injected to visualize morphant cells; 0.5–1 nl MOs/RNA mix was injected into one blastomere of 8- to 32-cell stage embryos.

Constructs Used

pCS2+ Centrin-GFP (Norden et al., 2009), pCS2+ H2B-RFP (Norden et al., 2009), pCS2+ EB3-GFP (Norden et al., 2009), pCS2+ PCNA GFP/RFP (Leung et al., 2011), and pCS2+ Ras-mKate2 (Weber et al., 2014) were used.

pCS2+ Ras-GFP was a kind gift from A. Oates (MRC); pCS2+ Centrin-tdTomato was a kind gift from D. Gilmour (EMBL), and HS-DN-N-Cadherin-mCherry was a kind gift from W.A. Harris (University of Cambridge).

This Study

pCS2+ EB3-mKate2, pCS2+ centrin-mKate2, HS-PCNA-GFP, HS-DN-Cep152-mKate2, HS-OS-Plk4-mKate2, HS-mKate2, HS-aPKC-CAAX-GFP, HS-Par3-GFP, HS-EB3-GFP, HS-DN-Plk1, HS-aPKC-CAAX-mKate2, HS-Ras-mKate2, HS-Utrophin-GFP, and HS-H2B-RFP were used.

Detailed cloning strategies for all of these constructs can be found in Supplemental Experimental Procedures.

Immunofluorescence

Embryos were fixed in 4% paraformaldehyde (PFA) for 8–12 hr. Whole-mount staining was carried out according to previously described protocols (Norden et al., 2009).

Primary Antibodies

Mouse anti-γ-tubulin (Sigma-Aldrich; 1:250), rat anti-pH3 (Abcam; 1:500), rabbit anti-pH3 (Chemicon, 1:500), rabbit anti-tRFP (Evrogen, 1:500), and mouse anti-ZO1 (Invitrogen 1:200) were used.

Secondary Antibodies

Alexa Fluor 488 donkey antirabbit, Alexa Fluor 488 chicken antimouse, Alexa Fluor 568 goat antirat, Alexa Fluor 594 goat antirabbit, Alexa Fluor 647 goat antirat, Alexa Fluor 647 goat antirabbit, Alexa Fluor 647 goat antimouse (all Molecular Probes, all 1:1,000) were used.

Additionally, for detection of GFP and RFP fluorophores, GFP booster and RFP booster (ChromoTech) were used (1:400 dilution). Nuclei were counterstained with 4',6-diamidino-2-phenylindole (DAPI) (1:5,000).

HS of Embryos

To induce expression from the HS promoter driven constructs, Petri dishes with 24–28 hpf embryos were placed in a 39°C water bath for 35 min and then returned to 28°C. Expression was observed ~2 hphs.

Image Acquisition and Analysis

In Vivo Time-Lapse Imaging

Embryos were anaesthetized using 0.04% MS-222 (Sigma) and mounted in 1% low melt agarose in E3 medium on Mattek glass bottom dishes. An Andor spinning disk system with a 63× water immersion objective (NA = 1.2) was used with a 30°C heating chamber; z stacks of 28–30 μm were collected, and optical sections in all experiments were 1 μm. Images were acquired every 5 min for 10–18 hr. For live imaging of DN-Plk1-expressing embryos, a Zeiss Lightsheet Z.1 microscope was used, with a Zeiss 63× water-dipping objective (numerical aperture [NA] = 1.0) and sample chamber heated to 28°C. Here z stacks of 60–90 μm were collected, with an optical section of 1 μm. Time-lapses were started ~32 hpf.

Confocal Scans

Imaging was performed on Zeiss LSM 510 or 710 confocal microscopes with a Zeiss 40× or 63× water-immersion objective (NA = 1.2). Image analysis was performed using ImageJ/Fiji software (NIH), and Matlab Software (MathWorks) was used to prepare graphs.

Laser Ablation

For laser ablation of apical centrosomes, an Andor spinning disk system with a 63× water-immersion objective (NA = 1.2) and a 1.6× OptoVar lens equipped with MicroPoint with a 15 Hz cutter laser with 405 nm dye cell was used. A square region of interest was drawn over an apical centrin signal. Ablation was performed in one z plane during live acquisition of single cells. Afterward, z stacks were acquired for 10–14 hr. Before each experiment, the MicroPoint set up was calibrated to ensure ablation as opposed to bleaching of centrin signal.

Drug Treatment

Blebbistatin (Enzo Life Sciences) was stored in DMSO at 20 mM. Embryos were dechorionated and transferred in 2 ml medium; 20 μl of the stock solution were added, and embryos were incubated for 1.5 hr at 28°C. Immediately after, they were mounted in 1% agarose and imaged or fixed in 4% PFA.

Embryos were mounted in 1% agarose at 30 hpf; 30 μl of 10 mM colcemide (Sigma-Aldrich) was added to 3 ml medium. Embryos were kept at 28°C, and image acquisition started 2 hr after drug addition.

RO3306 (ENZO Life Sciences) was stored as a 10 mM solution in DMSO and used at 125 μM. Embryos were kept at 28°C, and image acquisition was started 2 hr after drug addition.

Figure 7. Nonapical, Nonperpendicular Divisions Perturb Tissue Integrity and Early Neuronal Layering

(A) Confocal scans of a control embryo (left) and a HS-aPKC-CAAX-GFP injected embryo 24 hphs (right). Embryos were fixed at 50 hpf and stained with pH3 antibody. aPKC-CAAX expressing, mitotic cells can be observed at basal locations (arrows).

(B) Confocal scans of a control embryo injected with HS inducible cytosolic mKate2 (upper) and a HS-aPKC-CAAX-GFP injected embryo (lower) at 56 hpf/30 hphs. To visualize RGCs, the Tg(Ath5:GAP-RFP) line was used for aPKC-CAAX and Tg(Ath5:GAP-GFP) line for cytosolic mKate2 injection (RGCs, magenta). Control injected cells (green, upper) contribute to the intact RGC layer. In aPKC-CAAX expressing embryos the RGC layer features holes, filled by aPKC-CAAX (green) expressing cells (yellow boxes). See also Figure S4.

(C) Confocal scans of DN-Plk1 injected embryos stained with pH3 antibody (green) to visualize mitotic cells. DAPI is shown in magenta. DN-Plk1 expressing cells, arrested in mitosis, form an apical barrier. As a result, pH3-positive nuclei can be observed away from the apical surface (arrows: yellow open, subapical pH3; yellow filled, pH3 in the middle of the NE; cyan, basal pH3). HS was performed 11 hr prior to fixation.

(D) Time-lapse of cells in the embryo expressing DN-Plk1. DN-Plk1-positive cells coexpress H2B-RFP (magenta). To follow cell dynamics of nonmanipulated cells, H2B-GFP and Ras-GFP RNAs were injected mosaically (gray). Multiple non-DN-Plk1 cells can be observed dividing nonapically (arrows). Initially cells divide close to the apical barrier and maintain their apical process (yellow open arrows). Later in development, divisions occur at more basal locations (green, red, and blue arrows). HS was performed 11 hr prior to time-lapse. Time is in hr:min. The frames are from Movie S8. See also Figure S4.

(E) Confocal scans of Tg(Ath5:GAP-GFP) (green) embryos 53 hpf injected with DN-Plk1 and stained with pH3 antibody (magenta). pH3-positive nuclei can be observed at very basal locations (arrows). The RGC layer is disturbed in the central region of the retina, where the pH3-positive cells reside. HS was performed 29 hr prior to fixation. See also Figure S4.

Scale bars represent 10 μm. The dotted line represents the apical surface, and the solid line represents the basal side.

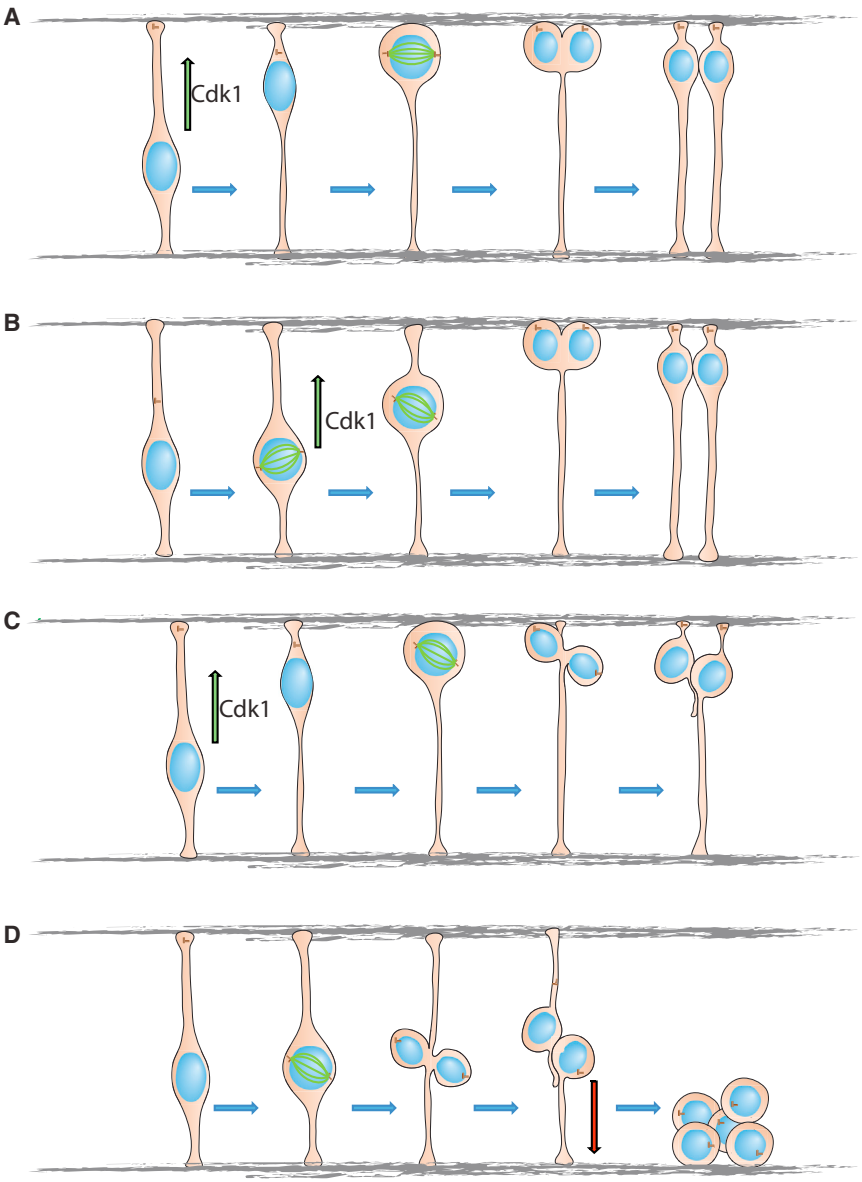

Figure 8. Schematic Summary of the Main Findings

(A) In WT conditions, divisions take place apically following apical IKNM and feature perpendicular cleavage planes.

(B) Following centrosome mispositioning and even in cases when nonapical mitotic entry occurs, apical IKNM is still initiated.

(C) Apical divisions with nonperpendicular cleavage planes in retinal NE of zebrafish do not cause impediment of apical cell attachments and thus do not perturb tissue integrity.

(D) Nonapical divisions impede cellular reintegration into the tissue. This results in cells losing their contact with the apical surface and forming basal cell clusters. Altogether, tissue integrity and architecture are perturbed.

PD166285 (Sigma) was stored as a 10 mM solution in DMSO and used at 50 μM. Embryos were kept at 28°C, and image acquisition started 2 hr after drug addition.

SUPPLEMENTAL INFORMATION

Supplemental Information includes Supplemental Experimental Procedures, four figures, and eight movies and can be found with this article online at http://dx.doi.org/10.1016/j.devcel.2014.12.001.

ACKNOWLEDGMENTS

We thank the Norden lab, J. Brugues, J. Mansfeld, J. Pines, J. Rink, M. Rujano, M. Thompson, and M. Zerial for discussion and helpful comments on the manuscript. C. Fröb, J. Icha, S. Schneider, and the MPI-CBG fish and light microscopy facility are thanked for experimental help. We also thank D. Cleveland, D. Gilmour, W.A. Harris, C.-P. Heisenberg, I. Hoffmann, E. Nigg, A. Oates, and S. Sokol for sharing constructs. P.J.S., I.P.W., and J.S. are members of the DIGS-BB PhD program. C.N. is supported by the Human Frontier Science Program (CDA-00007/2011) and the German Research Foundation (DFG) (SFB 655, A25; NO1068/1-1).

Received: April 9, 2014
Revised: October 7, 2014
Accepted: December 1, 2014
Published: January 15, 2015

REFERENCES

Basto, R., Lau, J., Vinogradova, T., Gardiol, A., Woods, C.G., Khodjakov, A., and Raff, J.W. (2006). Flies without centrioles. Cell *125*, 1375–1386.

Baye, L.M., and Link, B.A. (2007). Interkinetic nuclear migration and the selection of neurogenic cell divisions during vertebrate retinogenesis. J. Neurosci. *27*, 10143–10152.

Burkel, B.M., von Dassow, G., and Bement, W.M. (2007). Versatile fluorescent probes for actin filaments based on the actin-binding domain of utrophin. Cell Motil. Cytoskeleton *64*, 822–832.

Cayouette, M., and Raff, M. (2003). The orientation of cell division influences cell-fate choice in the developing mammalian retina. Development *130*, 2329–2339.

Cizmecioglu, O., Arnold, M., Bahtz, R., Settele, F., Ehret, L., Haselmann-Weiss, U., Antony, C., and Hoffmann, I. (2010). Cep152 acts as a scaffold for recruitment of Plk4 and CPAP to the centrosome. J. Cell Biol. *191*, 731–739.

Clark, B.S., Cui, S., Miesfeld, J.B., Klezovitch, O., Vasioukhin, V., and Link, B.A. (2012). Loss of Llgl1 in retinal neuroepithelia reveals links between apical domain size, Notch activity and neurogenesis. Development *139*, 1599–1610.

Coelho, P.A., Bury, L., Sharif, B., Riparbelli, M.G., Fu, J., Callaini, G., Glover, D.M., and Zernicka-Goetz, M. (2013). Spindle formation in the mouse embryo requires Plk4 in the absence of centrioles. Dev. Cell *27*, 586–597.

Cui, S., Otten, C., Rohr, S., Abdelilah-Seyfried, S., and Link, B.A. (2007). Analysis of aPKClambda and aPKCzeta reveals multiple and redundant functions during vertebrate retinogenesis. Mol. Cell. Neurosci. *34*, 431–444.

Das, T., Payer, B., Cayouette, M., and Harris, W.A. (2003). In vivo time-lapse imaging of cell divisions during neurogenesis in the developing zebrafish retina. Neuron *37*, 597–609.

Del Bene, F., Wehman, A.M., Link, B.A., and Baier, H. (2008). Regulation of neurogenesis by interkinetic nuclear migration through an apical-basal notch gradient. Cell *134*, 1055–1065.

Even-Faitelson, L., and Ravid, S. (2006). PAK1 and aPKCzeta regulate myosin II-B phosphorylation: a novel signaling pathway regulating filament assembly. Mol. Biol. Cell *17*, 2869–2881.

Fietz, S.A., and Huttner, W.B. (2011). Cortical progenitor expansion, self-renewal and neurogenesis-a polarized perspective. Curr. Opin. Neurobiol. *21*, 23–35.

Fisher, D., Krasinska, L., Coudreuse, D., and Novák, B. (2012). Phosphorylation network dynamics in the control of cell cycle transitions. J. Cell Sci. *125*, 4703–4711.

Godinho, L., Williams, P.R., Claassen, Y., Provost, E., Leach, S.D., Kamermans, M., and Wong, R.O.L. (2007). Nonapical symmetric divisions underlie horizontal cell layer formation in the developing retina in vivo. Neuron *56*, 597–603.

Grosse, A.S., Pressprich, M.F., Curley, L.B., Hamilton, K.L., Margolis, B., Hildebrand, J.D., and Gumucio, D.L. (2011). Cell dynamics in fetal intestinal epithelium: implications for intestinal growth and morphogenesis. Development *138*, 4423–4432.

Holland, A.J., Lan, W., Niessen, S., Hoover, H., and Cleveland, D.W. (2010). Polo-like kinase 4 kinase activity limits centrosome overduplication by autoregulating its own stability. J. Cell Biol. *188*, 191–198.

Hu, D.J.-K., Baffet, A.D., Nayak, T., Akhmanova, A., Doye, V., and Vallee, R.B. (2013). Dynein recruitment to nuclear pores activates apical nuclear migration and mitotic entry in brain progenitor cells. Cell *154*, 1300–1313.

Kishikawa, M., Suzuki, A., and Ohno, S. (2008). aPKC enables development of zonula adherens by antagonizing centripetal contraction of the circumferential actomyosin cables. J. Cell Sci. *121*, 2481–2492.

Kosodo, Y., Röper, K., Haubensak, W., Marzesco, A.-M., Corbeil, D., and Huttner, W.B. (2004). Asymmetric distribution of the apical plasma membrane during neurogenic divisions of mammalian neuroepithelial cells. EMBO J. *23*, 2314–2324.

Kosodo, Y., Suetsugu, T., Suda, M., Mimori-Kiyosue, Y., Toida, K., Baba, S.A., Kimura, A., and Matsuzaki, F. (2011). Regulation of interkinetic nuclear migration by cell cycle-coupled active and passive mechanisms in the developing brain. EMBO J. *30*, 1690–1704.

Lee, H.O., and Norden, C. (2013). Mechanisms controlling arrangements and movements of nuclei in pseudostratified epithelia. Trends Cell Biol. *23*, 141–150.

Leijen, S., Beijnen, J.H., and Schellens, J.H. (2010). Abrogation of the G2 checkpoint by inhibition of Wee-1 kinase results in sensitization of p53-deficient tumor cells to DNA-damaging agents. Curr. Clin. Pharmacol. *5*, 186–191.

Lénárt, P., Petronczki, M., Steegmaier, M., Di Fiore, B., Lipp, J.J., Hoffmann, M., Rettig, W.J., Kraut, N., and Peters, J.-M. (2007). The small-molecule inhibitor BI 2536 reveals novel insights into mitotic roles of polo-like kinase 1. Curr. Biol. *17*, 304–315.

Leung, L., Klopper, A.V., Grill, S.W., Harris, W.A., and Norden, C. (2011). Apical migration of nuclei during G2 is a prerequisite for all nuclear motion in zebrafish neuroepithelia. Development *138*, 5003–5013.

Liang, L., Haug, J.S., Seidel, C.W., and Gibson, M.C. (2014). Functional genomic analysis of the periodic transcriptome in the developing Drosophila wing. Dev. Cell *29*, 112–127.

McGowan, C.H., and Russell, P. (1995). Cell cycle regulation of human WEE1. EMBO J. *14*, 2166–2175.

Meyer, E.J., Ikmi, A., and Gibson, M.C. (2011). Interkinetic nuclear migration is a broadly conserved feature of cell division in pseudostratified epithelia. Curr. Biol. *21*, 485–491.

Miyata, T. (2008). Development of three-dimensional architecture of the neuroepithelium: role of pseudostratification and cellular 'community'. Dev. Growth Differ. *50* (*Suppl 1*), S105–S112.

Morin, X., Jaouen, F., and Durbec, P. (2007). Control of planar divisions by the G-protein regulator LGN maintains progenitors in the chick neuroepithelium. Nat. Neurosci. *10*, 1440–1448.

Murciano, A., Zamora, J., López-Sánchez, J., and Frade, J.M. (2002). Interkinetic nuclear movement may provide spatial clues to the regulation of neurogenesis. Mol. Cell. Neurosci. *21*, 285–300.

Nakajima, Y., Meyer, E.J., Kroesen, A., McKinney, S.A., and Gibson, M.C. (2013). Epithelial junctions maintain tissue architecture by directing planar spindle orientation. Nature *500*, 359–362.

Norden, C., Young, S., Link, B.A., and Harris, W.A. (2009). Actomyosin is the main driver of interkinetic nuclear migration in the retina. Cell *138*, 1195–1208.

Ossipova, O., Tabler, J., Green, J.B.A., and Sokol, S.Y. (2007). PAR1 specifies ciliated cells in vertebrate ectoderm downstream of aPKC. Development *134*, 4297–4306.

Pines, J., and Rieder, C.L. (2001). Re-staging mitosis: a contemporary view of mitotic progression. Nat. Cell Biol. *3*, E3–E6.

Poggi, L., Vitorino, M., Masai, I., and Harris, W.A. (2005). Influences on neural lineage and mode of division in the zebrafish retina in vivo. J. Cell Biol. *171*, 991–999.

Rakic, P. (1972). Mode of cell migration to the superficial layers of fetal monkey neocortex. J. Comp. Neurol. *145*, 61–83.

Rujano, M.A., Sanchez-Pulido, L., Pennetier, C., le Dez, G., and Basto, R. (2013). The microcephaly protein Asp regulates neuroepithelium morphogenesis by controlling the spatial distribution of myosin II. Nat. Cell Biol. *15*, 1294–1306.

Sauer, F.C. (1935). Mitosis in the neural tube. J. Comp. Neurol. *62*, 377–405.

Smits, V.A., Klompmaker, R., Arnaud, L., Rijksen, G., Nigg, E.A., and Medema, R.H. (2000). Polo-like kinase-1 is a target of the DNA damage checkpoint. Nat. Cell Biol. *2*, 672–676.

Spear, P.C., and Erickson, C.A. (2012). Apical movement during interkinetic nuclear migration is a two-step process. Dev. Biol. *370*, 33–41.

Tang, Z., Coleman, T.R., and Dunphy, W.G. (1993). Two distinct mechanisms for negative regulation of the Wee1 protein kinase. EMBO J. *12*, 3427–3436.

Taverna, E., and Huttner, W.B. (2010). Neural progenitor nuclei IN motion. Neuron *67*, 906–914.

Tsai, J.-W., Lian, W.-N., Kemal, S., Kriegstein, A.R., and Vallee, R.B. (2010). Kinesin 3 and cytoplasmic dynein mediate interkinetic nuclear migration in neural stem cells. Nat. Neurosci. *13*, 1463–1471.

Uberall, F., Hellbert, K., Kampfer, S., Maly, K., Villunger, A., Spitaler, M., Mwanjewe, J., Baier-Bitterlich, G., Baier, G., and Grunicke, H.H. (1999). Evidence that atypical protein kinase C-lambda and atypical protein kinase C-zeta participate in Ras-mediated reorganization of the F-actin cytoskeleton. J. Cell Biol. *144*, 413–425.

Vassilev, L.T. (2006). Cell cycle synchronization at the G2/M phase border by reversible inhibition of CDK1. Cell Cycle *5*, 2555–2556.

Weber, I.P., Ramos, A.P., Strzyz, P.J., Leung, L.C., Young, S., and Norden, C. (2014). Mitotic position and morphology of committed precursor cells in the zebrafish retina adapt to architectural changes upon tissue maturation. Cell Reports *7*, 386–397.

Wong, G.K.W., Baudet, M.L., Norden, C., Leung, L., and Harris, W.A. (2012). Slit1b-Robo3 signaling and N-cadherin regulate apical process retraction in developing retinal ganglion cells. J. Neurosci. *32*, 223–228.

Xie, Y., Jüschke, C., Esk, C., Hirotsune, S., and Knoblich, J.A. (2013). The phosphatase PP4c controls spindle orientation to maintain proliferative symmetric divisions in the developing neocortex. Neuron *79*, 254–265.